5 + Ph_3P was determined to be 1×10^{-3} M.

Preparation of the Methoxy Analogue of 4. To a solution of 167 mg (0.3 mmol) of 3 in 100 mL of $CHCl_3$ was added 100 mL of methanol with magnetic stirring. Upon the subsequent addition of 384 mg (1.47 mmol) of Ph_3P, the solution immediately became darker and then lightened in color over a 1–2-h period. Ten hours after the addition of Ph_3P, the solution was rotoevaporated to a yellow oil that when triturated with pentane, rotovapped, and dried under vacuum gave a yellow-white solid. The solid was extracted with 20 mL of Et_2O to remove unreacted Ph_3P and residual methanol. After rotoevaporation and drying under vacuum, 256 mg of a white solid was obtained. A portion of this was dissolved in $CDCl_3$, and sufficient Ph_3P was added to cause an upfield shift in the vinyl proton resonances which avoided obscuring the CHCl proton resonance of 4. Integration of the CHCl resonance of 4 vs. the methoxy analogue resonance gave a 85:15 molar ratio of methoxy analogue to 4. Following the combination of this NMR tube contents with the remainder of the white solid, the material was chromatographed on silica with $CHCl_3$. An early eluting fraction was determined by NMR spectroscopy to contain a mixture of 4 and methoxy analogue, while the major and later eluting fraction, following rotoevaporation, pentane trituration, and drying under vacuum, yielded 118 mg (46%) of the white methoxy analogue; mp 205 °C. Anal. Calcd for $C_{45}H_{43}OP_2Pt$: C, 60.59; H, 4.86. Found: C, 60.37; H, 4.92. Control experiments were run deleting either Ph_3P or MeOH resulting in no significant reaction according to NMR spectroscopy. In addition, solutions of 4 or 5 that were incubated in MeOH($CHCl_3$) showed no production of the methoxy analogues.

X-ray Structural Determination of 4. Crystals of 4 were grown at the interface of a heptane/chloroform bilayer and a specimen suitable for X-ray analysis was mounted on a fiber. X-ray data collection was carried out on a Nicolet R3m automated diffractometer equipped with a Mo target X-ray tube (λ = 0.71073 Å) and a graphite crystal monochromator.[8] Unit cell constants were determined to be a = 12.804 (5) Å, b = 13.061 (5) Å, c = 13.416 (5) Å, α = 65.95 (3)°, β = 67.59 (3)°, and γ = 8.45 (3)° for a cell of triclinic symmetry. The space group was determined to be $P\bar{1}$. Intensity measurements of 3669 independent reflections for $3 \leq 2\theta \leq 45°$ were observed with $I \geq 3\ \sigma(I)$. Absorption corrections were made by using the empirical psi scan method, and no decay corrections were necessary.

The structure was solved by direct methods that revealed the locations of all non-hydrogen atoms on the initial E map. The structure was refined to a final R value of 0.065 by a blocked-cascade technique with anisotropic thermal parameters for all non-hydrogen atoms. Hydrogen atoms were placed in idealized positions with isotropic thermal parameters. All structural determinations and refinement calculations were carried out with the SHELXTL package on the Nicolet R3m crystallographic system.[9] A cell mass of 1793.5 containing 892 electrons and two molecules per unit cell gave a calculated density of 1.60 g/cm^3 for $C_{44}H_{40}PtCl_2P_2$. The final difference map revealed no abnormal features.

Acknowledgment. We express our gratitude for financial support of this research by Montana State University and the National Science Foundation, Grant CHE 7826160. We also gratefully acknowledge work of Chuck Campana and the use of an R3m Crystallographic System provided by the Nicolet XRD Corp. Finally we wish to thank Dr. James Frye and the Colorado State University Regional NMR Center, funded the National Science Foundation (Grant CHE-78-18581) for obtaining the MAS/CP NMR spectra.

Registry No. 1, 3635-94-7; 2, 86834-41-5; 3, 86823-57-6; 4, 86823-58-7; 4 (MeO-deriv.), 86823-60-1; 5, 86823-59-8; $(C_2H_4PtCl_2)_2$, 12073-36-8; Ph_3P, 603-35-0.

Supplementary Material Available: Tables of bond lengths, bond angles, atom coordinates and temperature factors, anisotropic temperature factors, and hydrogen coordinates and temperature factors (5 pages). Ordering information is given on any current masthead page.

(8) Programs used for centering of reflections, autoindexing, refinement of cell parameters, axial photographs, and data collection were those described in: "Nicolet P3/R3 Data Collection Manual"; Calabrese, J. C., Ed.; Nicolet XRD Corp.: Fremont, CA, 1980.

(9) Programs used for data reduction, Fourier syntheses, direct method structure solution, least-squares refinement, error analysis, least-squares planes calculation, and calculation of hydrogen position are those described in: "Nicolet SHELXTL Structure Determination Manual"; Sheldreck, G. M., Ed.; Nicolet XRD Corp.: Fremont, CA, 1980.

(10) Cheng, A. K.; Stothers, J. B. *Org. Magn. Reson.* **1977**, *9*, 355.

Electronic and Geometric Features of (η^5-C_5H_5)ML 16-Electron Fragments. A Molecular Orbital Study of Ligand Effects

Peter Hofmann*† and Moothetty Padmanabhan

Institut für Organische Chemie der Universität Erlangen, D-8520 Erlangen, Federal Republic of Germany

Received March 9, 1983

Qualitative MO theory, based upon extended Hückel calculations, is utilized to study coordinatively unsaturated 16-electron fragments d^8 (η^5-C_5H_5)ML (M = transition metal, L = ligand) with respect to their geometric and electronic structure as a function of the ligands L. It is shown that such fragments, observed as reactive intermediates in organometallic reactions, can possess singlet ground states, which then will exhibit "nonlinear" Cp–M–L arrangements. The comparative ease of a number of important reactions proceeding via such intermediates without any spin-imposed high activation barriers can thus be readily understood.

Introduction

Since the early and important kinetic experiments by Basolo and Schuster-Woldan,[1] it has been well-known that d^8 18-electron half-sandwich compounds of the type (η^5-C_5H_5)M(CO)$_2$ (1, M = Co, Rh, Ir) undergo thermal ligand substitution reactions by associative (S_N2) pathways.[2] This puts them in contrast to metal carbonyl complexes

Scheme I

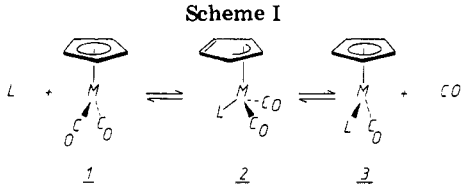

1 2 3

†To whom correspondence should be addressed at the Anorganisch-chemisches Institut der Technischen Universität München, D-8046 Garching, FRG.

0276-7333/83/2302-1273$01.50/0

Scheme II

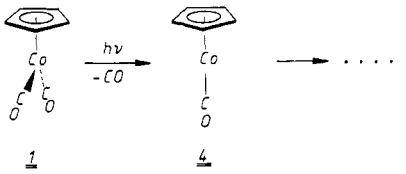

Scheme III

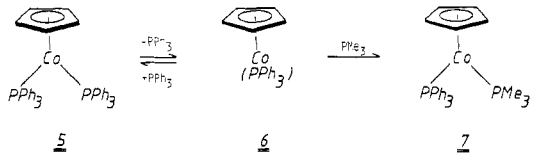

Scheme IV

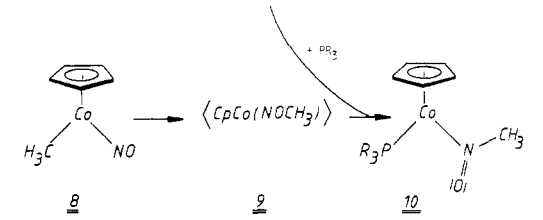

like $Ni(CO)_4$, $Fe(CO)_5$, $Cr(CO)_6$, etc., which typically react by CO loss[3] via "unsaturated" (more or less solvent stabilized) 16-electron intermediates, as exemplified by $Cr(CO)_5$.[4] The mechanism at present believed to be operative for dicarbonyl species $CpM(CO)_2$ (**1**, Cp = η^5-C_5H_5) is shown in Scheme I. Any d^8 $CpM(CO)$ intermediates do not seem to be involved. The accessibility of (η^3-C_5H_5)$M(CO)_2L$ transition states or intermediates **2**, formed by nucleophilic attack of L at the metal, avoids unfavorable 20-electron configurations through a simple "slipping" motion of the ML_n fragment.[5] Indeed on the basis of further experimental evidence[6] a general rule has been suggested by Basolo recently,[7] saying that associative substitution mechanisms will play a role whenever the metal can localize a pair of electrons onto an appropriate ligand,[8] as shown for Cp in **2**. Contrastingly, there have been several reports in the recent literature that convincingly indicate a thermally or photochemically induced formation of 16-electron intermediates of the d^8 CpML type. Years ago Brintzinger[9] had postulated the formation of an intermediate CpCo(CO) (**4**) in solution photochemistry experiments on the parent dicarbonyl $CpCo(CO)_2$ (Scheme II). The monocarbonyl **4** was reported to undergo fast transformations to a number of binuclear and trinuclear complexes. A more recent reinvestigation[10] of the photochemistry of **1**, although in inert-gas matrices (Ar, N_2), seems to indicate, however, that no CpCo(CO) (**4**) is formed at all and that Brintzinger's intermediate may really have been the dinitrogen complex $CpCo(CO)(N_2)$ (**3**, L = N_2). Moreover, these matrix isolation studies revealed that in a CO matrix a species is reversibly formed by irradiation, the vibrational spectra of which can be plausibly interpreted by assuming the presence of a $Co(CO)_3$ subunit, consistent with an association of carbon monoxide to **1**, yielding (η^3-C_5H_5)$Co(CO)_3$ (**2**, L = CO) in agreement with Basolo's "rule".

Interestingly, the recent past has brought even more experimental observations, which clearly demonstrate that d^8 CpML fragments with 16 valence electrons do indeed exist as reactive intermediates. For the case of $CpIr(CO)_2$, Rausch[11] has postulated the formation of CpIr(CO) as the active species formed on photolysis of the dicarbonyl. Similarly Werner and Leonhard[12] have pointed out the intermediacy of a related 16-electron fragment, $CpCo(PMe_3)$, generated via PMe_3 abstraction from $CpCo(PMe_3)_2$ by the "masked" Lewis acid $CpMn(CO)_2(THF)$. In addition their experiments indicate the generation of CpCo(CO) from $CpCo(CO)_2$ in an analogous fashion. Cp*Ir(CO) (Cp* = η^5-C_5Me_5) was found by Graham et al.[13] recently in photochemical studies of $Cp^*Ir(CO)_2$ and was shown to be capable of oxidatively adding to CH bonds of saturated hydrocarbons. Bergman and Janowicz[14] generated the unsaturated fragment $Cp^*Ir(PPh_3)$ from $Cp^*Ir(PPh_3)H_2$ by light-induced H_2 loss; again this species is able to insert into CH bonds of hydrocarbons. In a similar study, Jones and Feher[15] claimed to have obtained $Cp^*Rh(PMe_3)$ as an intermediate product from $Cp^*Rh(PMe_3)$(aryl)H molecules both by thermal and photochemical reactions. Even more fascinating and intriguing is the observation by Shapley and co-workers,[16] that $CpIr(CO)H_2$ is clearly in thermal equilibrium with H_2 and CpIr(CO), which can be trapped by appropriate ligands or causes the formation of $Cp_3Ir_3(CO)_3$.

We became especially interested in this context by yet another paper from the Bergman group,[17] which essentially formed the impetus for this study. Prompted by a prediction of Collman,[18] that ligand dissociations in d^8 $CpML_2$ complexes might be spin forbidden, e.g., should possess abnormally high barriers (thus offering a rationale for preferred associative pathways), these authors carried out a kinetic study of phosphine substitution in $CpCo(PPh_3)_2$ (**5**). The objective was to test the validity of the assumption that intermediates of the CpML type should be forced by symmetry to have a triplet ground state for a d^8 electron count and should therefore not be easily accessible as intermediates in thermal organometallic reactions. Similar arguments of a spin-induced high barrier

(1) Schuster-Woldan, H.-G.; Basolo, F. *J. Am. Chem. Soc.* **1966**, *88*, 1657.
(2) For a recent review see: Basolo, F. *Coord. Chem. Rev.* **1982**, *43*, 7.
(3) Werner, H. *Angew. Chem.* **1968**, *80*, 1017; *Angew. Chem., Int. Ed. Engl.* **1968**, *7*, 930.
(4) Electronic structure calculations: Hay, P. J. *J. Am. Chem. Soc.* **1978**, *100*, 2411 and references therein.
(5) For a general analysis of ML_n shift processes (haptotropic shifts) in complexes see: Albright, T. A.; Hofmann, P.; Hoffmann, R.; Lillya, C. P.; Dobosh, P. A. *J. Am. Chem. Soc.* **1983**, *105*, 3396. Anh, N. T.; Hoffmann, R. *Ibid.* **1978**, *100*, 110.
(6) Chang, C. Y.; Johnson, C. E.; Richmond, T. G.; Chen, Y. T.; Trogler, W. C.; Basolo, F. *Inorg. Chem.* **1981**, *20*, 3167.
(7) Basolo, F. *Inorg. Chim. Acta* **1981**, *50*, 65. For a theoretical generalization see: Chu, S.-Y.; Hoffmann, R. *J. Phys. Chem.* **1982**, *86*, 1289.
(8) $Cp_2W(CO)_2$, a formal 20-electron complex, exhibits this localization in its ground-state structure with one Cp ring being η^3 bound: Huttner, G.; Brintzinger, H. H.; Bell, L. G.; Friedrich, P.; Bejenke, V.; Neugebauer, D. *J. Organomet. Chem.* **1978**, *145*, 329. Other cases of ground-state localization of a pair of electrons on a Cp ring include Pd_2L_2 (μ-Cp)(μ-X), Pd_2L_2 (μ-Cp)$_2$, or CpPdR(PR)$_3$ molecules: Werner, H. *Adv. Organomet. Chem.* **1981**, *19*, 155. Werner, H.; Kraus, H.-J.; Schubert, U.; Ackermann, K.; Hofmann, P. *J. Organomet. Chem.* **1983**, *250*, 517.
(9) Lee, W.-S.; Brintzinger, H. H. *J. Organomet. Chem.* **1977**, *127*, 87.
(10) Crichton, O.; Rest, A. J.; Taylor, D. J. *J. Chem. Soc., Dalton Trans.* **1980**, 167.
(11) Rausch, M. D.; Gastinger, R. G.; Gardener, S. A.; Brown, R. K.; Wood, J. S. *J. Am. Chem. Soc.* **1977**, *99*, 7870.
(12) Leonhard, K.; Werner, H. *Angew Chem.* **1977**, *89*, 656; *Angew. Chem., Int. Ed. Engl.* **1977**, *16*, 649.
(13) Hoyono, J. K.; Graham, W. A. G. *J. Am. Chem. Soc.* **1982**, *104*, 3723.
(14) Janowicz, A. H.; Bergman, R. G. *J. Am. Chem. Soc.* **1982**, *104*, 352.
(15) Jones, W. D.; Feher, F. J. *J. Am. Chem. Soc.* **1982**, *104*, 4240.
(16) Shapley, J. R.; Adair, P. C.; Lawson, R. J.; Pierpoint, C. G. *Inorg. Chem.* **1982**, *21*, 1701.
(17) Janowicz, A. H.; Bryndza, H. E.; Bergman, R. G. *J. Am. Chem. Soc.* **1981**, *103*, 1516.
(18) See footnote 5 in ref 17. We are also grateful to Prof. Collman for bringing this prediction to our attention: Collman, J. P., private communication.

have been forwarded by Collman and Hegedus[19] for reactions involving d^2 Cp_2ML complexes, although experimental evidence for Cp_2W–$C_2H_5^+$ is available.[20] Cp_2ML systems have been studied theoretically by Hoffmann and Lauher[21] and for a d^2 electron count might well deviate from C_{2v} symmetry, the assumption of which led to Collman's proposal. For systems like the monocarbonyl **4**, C_{5v} symmetry assumed, high-spin character is indeed strictly required as can be easily seen from the orbital pattern of a d^8 CpM conical fragment[22] interacting with a carbonyl ligand (vide infra).

Surprisingly, Bergman found that the substitution of PPh_3 in **5** by PMe_3, leading to the mixed bis(phosphine) system **7**, not only rapidly takes place at very low temperature but also definitely involves the formation of $CpCo(PPh_3)$ (**6**) in the rate-determining *dissociative* step (Scheme III). Intermediate **6** is then irreversibly trapped by PMe_3 in a very fast second step.

A final piece of evidence for CpML 16-electron intermediates to be cited here is found in Bergman's investigation of an NO insertion reaction as shown in Sheme IV.[23] From kinetic data it was concluded that **9**, whatever its detailed structure may be, is easily formed from **8** in a rate-determining step and is then intercepted by added phosphine in a fast consecutive reaction yielding **10**.

With all the above cited evidence available, we thought it worthwhile to take a closer look at the electronic structure of some d^8 CpML model systems. It is unclear what geometry and which spin state is to be expected for such fragments, and it is the purpose of this paper to decipher some of the dominant molecular orbital features that play a role in determining their structures and their tendency toward singlet or triplet ground states. Incidentally, d^8 CpML species probably also are important intermediates in the well-documented alkyne oligomerizations mediated for instance by $CpCo(CO)_2$[24] and $CpCo(PR_3)_2$.[25]

Obviously species like **4**, "linear" CpCo(CO), C_{5v}, in contrast to the 18-electron analogues CpNi(NO)[26] or $CpCu(PR_3)$,[27] are bound to be Jahn–Teller unstable if they were to adopt a single ground state ($^1E_2$). As already speculated by Bergman,[17] this fact might lead to a preferred "bent" ground-state geometry for isoelectronic phosphine-containing fragments like **6** or like CpRh(PMe_3), Cp*Ir(PPh_3), etc., allowing these intermediates to stay on the singlet (low-spin) surface, thus circumventing any spin-forbiddenness problems for reactions passing through d^8 CpML species. We have discussed the electronic structure of "bent" d^8 CpM(CO) fragments as building blocks of metal–metal bonded systems elsewhere.[28] They are isoelectronic to $Fe(CO)_4$, for which a triplet ground state was found in matrix isolation studies.[29]

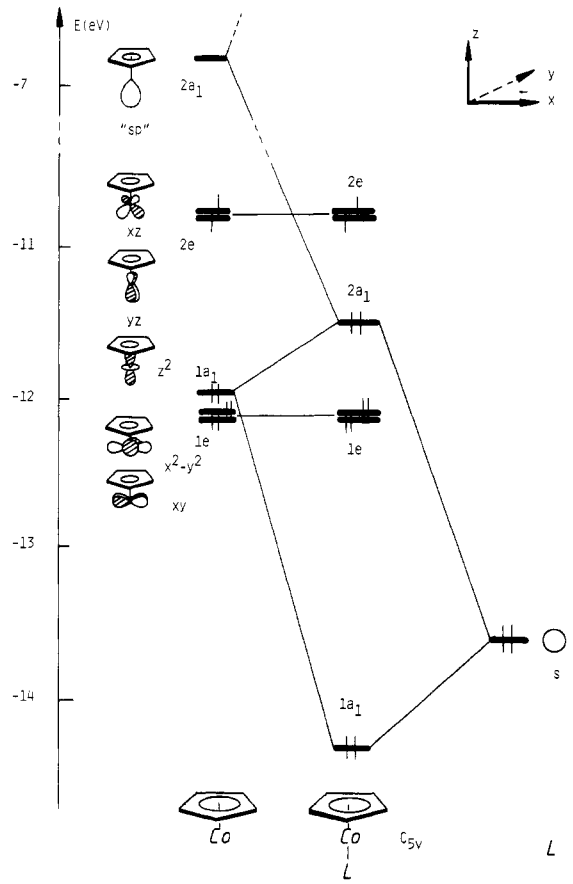

Figure 1. Orbital interaction diagram for a model system CpCoL (L = σ donor, "linear" C_{5v} geometry). Only the metal contributions to the wave functions of CpCo are shown. The numbering of the symmetry labels of MO levels corresponds to only the valence levels here and in all following cases.

Here we make use of extended Hückel calculations[30] to inspect more closely the orbital structure of various d^8 CpML systems as a function of L and its electronic properties. Although our calculations using the EH methodology will of course not allow us to determine absolute energies for singlet vs. triplet states,[31] they should provide guidelines for a general qualitative analysis of geometric and electronic features in CpML species.

In the following section we discuss the electronic structures of d^8 CpML fragments for different prototypes of ligands L.

Results and Discussion

d^8 CpML (L = σ Donor). Let us start with ligands having rotational symmetry (linear, monoatomic, C_{3v}, etc.) and here with the simplest case of a CpML system, where

(19) Collman, J. P.; Hegedus, L. S. "Principles and Applications of Organotransition Metal Chemistry"; University Science Books: Mill Valley, CA, 1980.
(20) Hayes, J. C.; Pearson, G. D. N.; Cooper, N. J. *J. Am. Chem. Soc.* **1981**, *103*, 4648.
(21) Lauher, J.; Hoffmann, R. *J. Am. Chem. Soc.* **1976**, *98*, 1729 and references cited therein.
(22) Elian, M.; Chen, M. M. L.; Mingos, D. M. P.; Hoffmann, R. *Inorg. Chem.* **1976**, *15*, 1148.
(23) Weiner, W. P.; White, M. A.; Bergman, R. G. *J. Am. Chem. Soc.* **1981**, *103*, 3612.
(24) For a review see: Vollhardt, K. P. C. *Acc. Chem. Res.* **1977**, *10*, 1 and references therein. Vollhardt, K. P. C.; Bergmann, R. G. *J. Am. Chem. Soc.* **1974**, *96*, 4996.
(25) Yamazaki, H.; Wakatsuki, Y. *J. Organomet. Chem.* **1977**, *139*, 157. Wakatsuki, Y.; Kuramitsu, T.; Yamazaki, H. *Tetrahedron Lett.* **1974**, 4549. McAlister, D. R.; Bercaw, J. E.; Bergman, R. G. *J. Am. Chem. Soc.* **1977**, *99*, 1666.
(26) Fischer, E. O.; Jira, R. *Z. Naturforsch., B: Anorg. Chem., Org. Chem., Biochem., Biophys., Biol.* **1954**, *98*, 518. Cox, A. P.; Thomas, L. F.; Sheridan, J. *Nature (London)* **1958**, *181*, 1157.
(27) Cotton, F. A.; Takats, J. *J. Am. Chem. Soc.* **1970**, *92*, 2353.
(28) Hofmann, P. *Angew. Chem.* **1979**, *91*, 591; *Angew. Chem., Int. Ed. Engl.* **1979**, *18*, 554. Pinhas, A. R.; Albright, T. A.; Hofmann, P.; Hoffmann, R. *Helv. Chim. Acta* **1980**, *63*, 29.
(29) Poliakoff, M.; Turner, J. J. *J. Chem. Soc., Dalton Trans.* **1974**, 2276. Barton, T. J.; Grinter, R.; Thomson, A. J.; Davies, B.; Poliakoff, M. *J. Chem. Soc., Chem. Commun.* **1977**, 841. For MO-based predictions see: Burdett, J. K. *J. Chem. Soc., Faraday Trans. 2* **1974**, *70*, 1599. The molecule is of C_{2v} symmetry.
(30) Hoffmann, R. *J. Chem. Phys.* **1963**, *39*, 1397. Hoffmann, R.; Lipscomb, W. N. *Ibid.* **1962**, *36*, 3179, 3289; **1962**, *37*, 2872.
(31) The reader should recall here the long history and difficulties (and costs) encountered in *quantitatively reliable* calculations of singlet–triplet splittings even for simple organic species like carbenes or carbene analogues. For a practically complete summary of semiempirical and ab initio work on carbenes see for example: Davidson, E. R. In "Diradicals"; Borden, W. T., Ed.; Wiley: New York 1982; Chapter 2.

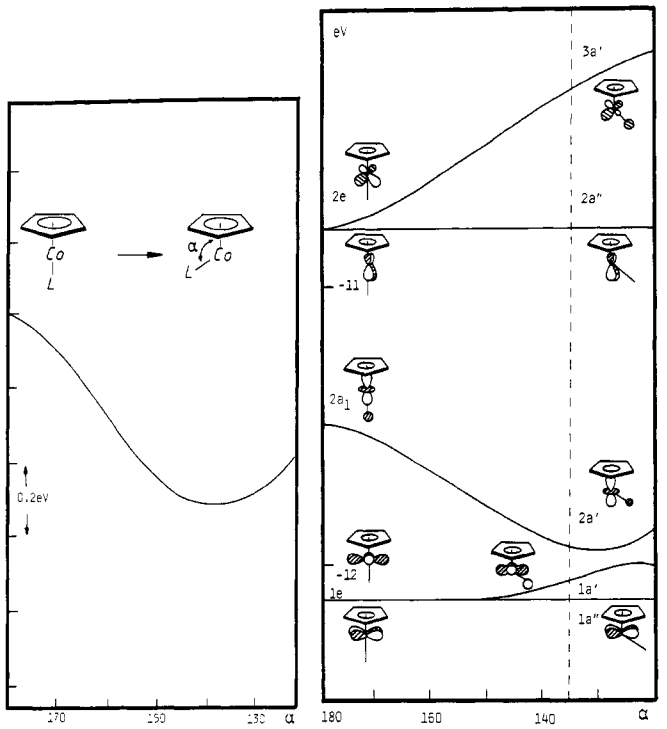

Figure 2. Walsh diagram and total energy variation for the transformation **11** → **12** (C_{5v} → C_s). The bending here and in all other cases (unless otherwise noted) is in a mirror of the Cp ring. The asymmetry of total energy curves or Walsh diagrams induced by bending either toward the unique carbon of Cp or toward a C–C bond on the opposite side is only minute, in accordance with a minute rotational barrier.

L is a pure σ donor. We can model such a group by a hydride-like pseudoligand L carrying a single 1s-type function occupied by two electrons. With Co as the metal center, d^8 CpML (**11**) is a model for phosphine systems like $CpCo(PPh_3)$ (**6**) or $CpCo(PMe_3)$. We can disregard for the moment any potential acceptor capability of real phosphine ligands, which, however, will be added to our analysis later. The orbital structure of C_{5v} "linear" CpCoL is shown in Figure 1, the interaction diagram between a conical d^8 CpCo fragment and L ($L = H^-$). The valence orbitals of C_{5v} CpCo have been discussed in the literature[22] and need not be reiterated here.

The s-type donor orbital of L interacts only with $2a_1$, an empty hybrid at the metal center of CpCo with predominant sp character, and also with $1a_1$, mainly z^2.[32] The latter is destabilized by the ligand orbital, and the antibonding combination of both levels mixes into itself $2a_1$, in a bonding way toward L. Both e sets of CpCo (1e ($x^2 - y^2$,xy) and 2e (xz,yz)) cannot interact with L by symmetry. Electronically a triplet ground state is mandatory for this geometry. An obvious escape from this situation would be possible by bending **11** to a structure shown in **12**. Let us see what happens to the one-electron levels

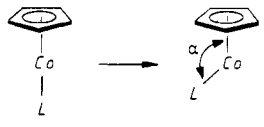

11 **12**

of Figure 1, if we go from **11** to **12**. The results of a model calculation for our pseudoligand L are presented in the Walsh diagram of Figure 2. Also shown is the total energy change for a closed-shell configuration as a function of the bending angle α. In the reduced symmetry of **12** (C_s) both former e sets (1e, 2e) split as α decreases from 180°. While yz of 2e (2a'' in Figure 2) is unaffected by the bending motion (L moves on the nodal plane), xz (3a') is destabilized because the antibonding interaction with the donor level of L is now turned on. The lifting of degeneracy brings out a noticeable HOMO–LUMO gap for the minimum energy structure of the low-spin case (yz doubly occupied). The HOMO 2a'' is pure yz of the CpCo fragment while the LUMO 3a' is mainly composed of xz, $2a_1$, and the s-type orbital of L as schematically indicated in **13**. **13**, the σ acceptor level of bent CpML, is nicely hybridized toward the missing ligand of a parent $CpML_2$ molecule. The dominant energetic stabilization upon bending comes from $1a_1$ (z^2) of CpCo, which had been interacting with the donor function of L in C_{5v} in an antibonding fashion as shown in Figure 1. The donor orbital of L moves toward the nodal cone of z^2 upon bending, and the strong antibonding interaction is reduced. In addition xz can now mix into this level in a bonding way from above, while the interaction of L with the well-hybridized $2a_1$ of CpCo is not perturbed very much. The z^2-derived level 2a' therefore drastically drops in energy, finally undergoing an avoided crossing (see Figure 2) with 1a' ($x^2 - y^2$), which is increasingly destabilized by bending, because it feels more and more antibonding from L. The changes in overlap on bending for z^2 and $x^2 - y^2$ with s of L are indicated in **14** and **15**; 1a'' (xy) of course stays put for the same reason as 2a'' (yz).

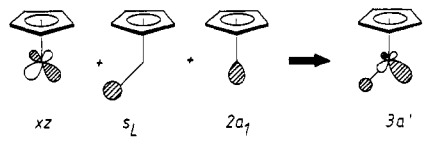

13

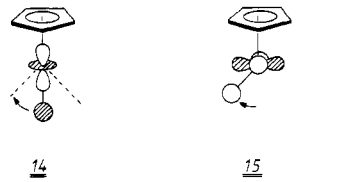

14 **15**

For our specific choice of L as H^- with $H_{ii} = -13.6$ eV, low-spin CpCoL is more stable in the bent geometry by about 12 kcal/mol, α being about 137°. Of course for the 18-electron case with two more electrons in the Walsh diagram of Figure 2, a "linear" geometry will be preferred, and this is exactly what has been found for $CpCu(PR_3)$.[27] The bent structure displays a HOMO–LUMO gap of 0.51 eV between the formerly degenerate levels 3a' and 2a'' with xz and yz character. We cannot conclude from this number that any d^8 CpML (L = σ donor) *must* be a bent singlet structure in its ground state, but we can say that by adopting or retaining a bent configuration (say after dissociation of one group L from a $CpML_2$ precursor), a d^8 CpML fragment has a chance to stay on the singlet surface until it gets trapped. A symmetry-imposed high-spin situation due to a linear structure can thus well be avoided. This just might be the case for Bergman's intermediate $CpCo(PPh_3)$, thus explaining its ready formation by ligand dissociation from $CpCo(PPh_3)_2$ at low temperature. The chance for a CpML system to remain on the singlet surface in a one-electron picture will depend on the actual size of the HOMO–LUMO gap of the bent structure and the gain in total energy upon bending, both being a function of the

(32) For simplicity we use the shorthand notation z^2, $x^2 - y^2$, xy, xz, yz, x, y, and z for d_{z^2}, $d_{x^2-y^2}$, ..., p_x, p_y, and p_z orbitals, respectively.

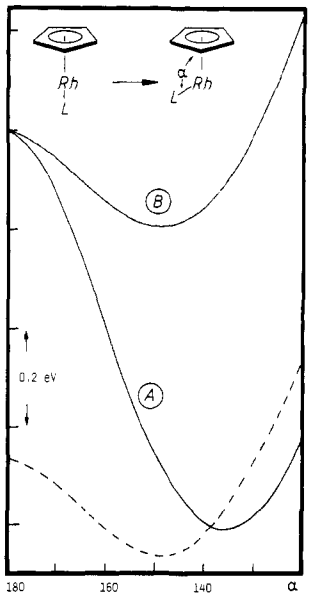

Figure 3. Total energy curves for bending of CpRhL (L = σ donor): curve A, 2a″ doubly occupied; curve B, 2a″ and 3a′ each singly occupied; dotted line, see text.

specific ligand L. The second determining factor, then, is the spin pairing energy of the metal, which, depending on the 3a′–2a″ gap, may decide the system's choice for a singlet or a triplet ground state.

The Walsh diagram of Figure 2 is very reminiscent of the analogous situation for the organic "six-electron fragment" CH_2[33] and of carbenes in general, which are of course isolobal to a bent d^8 CpML.[34] This may imply that, as in the case of CH_2, a triplet system should also have a nonlinear (Cp–M–L) arrangement, though less bent than the singlet. Figure 3 shows the total energy change on bending as it derives from the Walsh diagram of Figure 2, if the two orbitals emerging from 2e (2a″ and 3a′) are each occupied by one electron (curve B). Curve A, the total energy change for 2a″ doubly occupied, analogous to Figure 2, is given for comparison. After the redistribution of the two relevant electrons, the bending angle α increases to 148°, the one-electron level based total energy gain on bending is much smaller than for the $(2a'')^2$ occupation pattern. The values for Figure 3 are taken from calculations on CpRhL in order to exhibit the situation also for the heavier relative of cobalt, where an analogous picture exists. Both curves A and B, representing only the sum of EH orbital energy changes, of course, start out from the same energy for the linear C_{5v} geometry, as our EHT model calculations do not take into account spin properties and mutual interactions of electrons. In reality the spin pairing energy will cause the triplet curve B to start out from a lower energy than curve A. If this shift is large enough to put the triplet minimum below that of the singlet (large spin pairing energy, dotted curve in Figure 3), then the ground state of a d^8 CpML would be a bent triplet.

It is clear that rigorous calculations, yielding reliable, fully geometry-optimized singlet and triplet energy values, comparable in quality to, say, state of the art CH_2 results, would involve an enormous computational effort and might even be not feasible at the present time. We resist the temptation here to derive any numeric values for state

Table I. Geometric and Electronic Changes of σ-Donor Systems on Bending

CpML	α,[a,b] deg	energy gain on bending,[b] eV	HOMO-LUMO gap, eV
CpCoL[c]			
H_{ii}(L) = −12.0 eV	46.5	0.75	0.65
−13.6 eV	43.5	0.52	0.50
−15.0 eV	42.0	0.43	0.44
$CpCo(PH_3)$[d]	33.0	0.13	0.25
$CpRh(PH_3)$[d]	38.0	0.30	0.43
$CpCo(CH_3)^-$	43.0	0.57	0.54
$CpRh(CH_3)^-$	44.5	0.74	0.72

[a] Angle corresponding to minimum energy. [b] For "singlet" model, i.e., 2a″ doubly occupied. [c] L is the model donor ligand with 1s function, see text. [d] No d orbitals on P.

energies via the usual approach, which would involve spin pairing energies and electron interaction parameters for the d^8 metals in question here,[35] because we believe that such a ligand field type treatment superimposed upon EH calculations would not be very reliable either.[36]

From the well-known decrease of spin pairing energies within the Co, Rh, and Ir triad we can conclude, however, that the heavier metal atom systems d^8 CpML (L = σ donor as above) stand a better chance to exist as bent singlet species than their cobalt counterparts.

Up to now we have made an arbitrary choice for our model donor ligand L, simply by using an ionization potential for the 1s function of −13.6 eV. Let us analyze next, how a variation in the σ donor character of L will influence our picture. We can, to a first approximation, mimic a better or worse σ donor L by decreasing or increasing the orbital energy (H_{ii} value) of L. The changes induced by such a variation, which we see for our purely σ-interacting pseudoligand L, of course, carry over to other types of ligands, where the σ donor capability is underlying any additional π donor or π acceptor interactions between M and L, which we will turn to later on.

As can be seen from Figure 1, a higher lying donor orbital of L will lead to a more strongly destabilized $2a_1$ level of CpML in the linear geometry, closer in energy to the half-filled 2e set. Bending of CpML for a better donor, therefore, should lead to a stronger stabilization of this level and in turn also to an increased destabilization of 3a′ (xz), compared to the Walsh diagram in Figure 2. In terms of intramolecular perturbation theory[37] a better donor leads to a stronger mixing and repulsion of 3a′ (xz) and 2a′ (z^2) as soon as bending occurs. As a result, more energy will be gained on going from C_{5v} to C_s and the gap between 3a′ and 2a″ of the minimum structure of a bent singlet should increase with increasing donor capability of L. Opposite effects have to be expected for weaker σ donors. Figure 4 shows the computed total energy curves and orbital energy changes for three different orbital energies of the 1s function of L. The expected trends emerge from the model calculations: the best donor induces the highest energetic preference for a bent singlet structure (cf. Table I); 2a′ here experiences the largest stabilization and 3a′ gets

(33) See for example: Gimarc, B. M. "Molecular Structure and Bonding": Academic Press: New York, 1979.
(34) Hoffmann, R. *Science (Washington, DC)* **1981**, *211*, 995. Hoffmann, R. *Angew. Chem.* **1982**, *94*, 725; *Angew. Chem., Int. Ed. Engl.* **1982**, *21*, 711.
(35) Slater, J. C. "Quantum Theory of Atomic Structures"; McGraw-Hill: New York, 1960; Vol. I. Williams, A. F. "A Theoretical Approach to Inorganic Chemistry"; Springer-Verlag: Berlin, 1979. Griffith, J. S. "The Theory of Transition Metal Ions", Cambridge University Press: Cambridge, 1961.
(36) In this connection see: Vanquinkenborne, L. G.; Haspeslagh, L. *Inorg. Chem.* **1982**, *21*, 2448.
(37) Libit, L.; Hoffmann, R. *J. Am. Chem. Soc.* **1974**, *96*, 1370 and references therein.

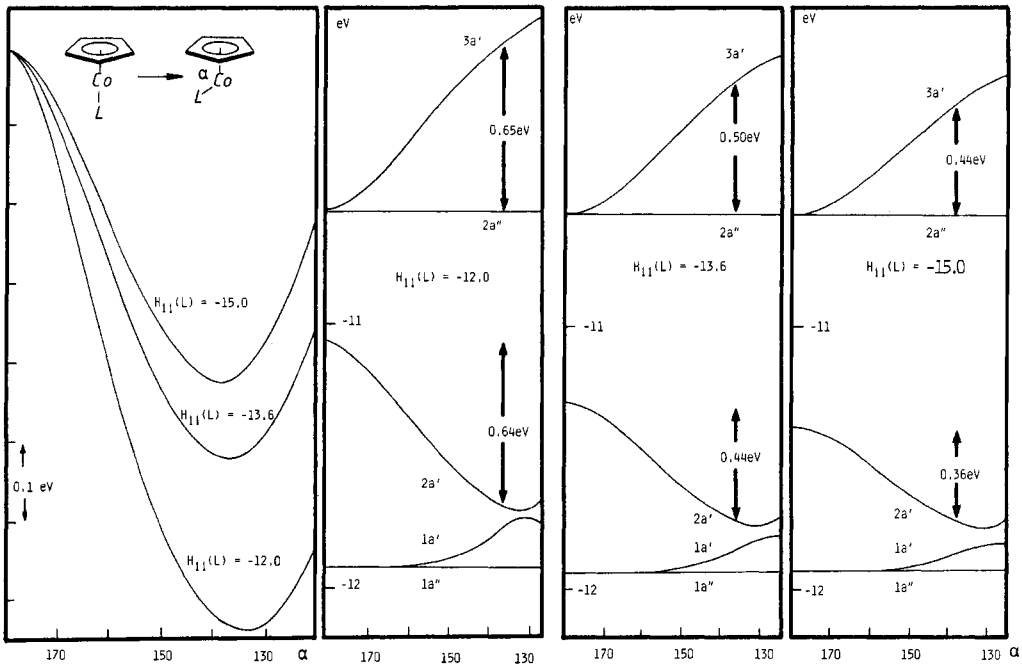

Figure 4. Total energy changes and corresponding Walsh diagrams for bending CpCoL (L = σ donor, 2a" doubly occupied). The different H_{ii} values used for the model ligand's 1s function are given in each diagram as well as HOMO–LUMO gaps and $2a_1$ stabilization energies at the C_s minimum energy structures.

destabilized most. Of course not only the energetic position of the donor orbital of L is of importance. As suggested by the standard perturbation expresssion,[38] governing the interaction of two MO levels, the overlap also plays a decisive role. The trends here can be tested by changing the exponent of the 1s function of the model ligand L, and parallel effects to changing the orbital electronegativity are caused. The larger the overlap of the donor orbital with xz (in C_s) and z^2 (in C_{5v}), the more preference toward a bent singlet results. The overlap situtation on the other hand is also influenced by the nature of the metal. The heavier metals (Rh, Ir) should also, from that point of view, be better candidates for a bent singlet structure than their cobalt analogues.

We have also performed model calculations for somewhat more realistic donor ligands L with sp^3-type donor levels. Examples are $CpCo(PH_3)$, $CpCo(CH_3)^-$, $CpRh(PH_3)$, and $CpRh(CH_3)^-$ (with an s,p basis for P), and we see the same trends as noted above. The bent geometry is preferred, and the HOMO–LUMO gap depends on the energetic position of the ligand lone pair. We do not present the results here in detail, as they are parameter dependent with respect to the actual numbers, but we note that the methyl group as the better donor leads to stronger stabilization upon bending and to a larger frontier orbital gap (see Table I).

Having understood the general picture for d^8 CpML systems with L as pure σ donors, we now turn to more complex ligand types. Actually $CpM(PH_3)$ molecules as models for $CpM(PR_3)$ systems already take us to a point, where one has to worry about additional effects of acceptor orbitals of PR_3 upon structure and possible spin states, as they certainly play a role in real phosphine ligands. (The acceptor levels here may be d AOs on P or σ^* levels of the P–R bonds of PR_3.)

d^8 CpML (L = π Acceptor). Let us first consider a clear-cut and typical back-bonding situation, a linear and "double-faced" π acceptor ligand, the CO molecule. In Figure 5a the interaction diagram between CpCo and CO in C_{5v} symmetry is given, the two π^* orbitals of the CO ligand are seen to interact with 2e (xz,yz) of CpCo, bringing the half occupied 2e set of the linear structure energetically close to $2a_1$ (z^2), which is destabilized by the nonbonding donor level n of CO. The 1e set of CpCo behaves as in the pure σ donor case discussed above, not interacting with the ligand functions. The Walsh diagram for bending to C_s is shown in Figure 5b. Again 2e splits into two levels, and 3a' (xz) is destabilized by turning on σ antibonding with n *and* additionally by loss of π interaction with the appropriate π^* orbital of CO. The yz member of 2e, 2a", in this case, does not stay unaffected but is also going up in energy due to its reduced back-bonding to the other π^*-acceptor level of the CO group. The relevant changes in character for the two frontier levels 3a' and 2a" are indicated in **16** and **17**. As 2a" suffers much less than 3a' from its weakened interaction with π^* of CO and does not begin to feel antibonding interaction with n, its ascent in energy is much less pronounced than that of 3a'.

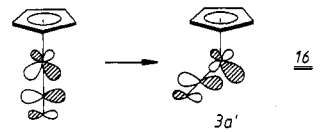

16

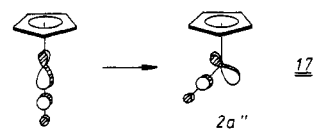

17

The reduced (C_s) symmetry finally again leads to some mixing of z^2 (and of $x^2 - y^2$, s, x, z) into 3a' and of some xy (and y) character into 2a", rehybridizing these MO's as indicated in **16** and **17**. It is these two frontier levels, **16** and **17**, that allow one to view CpCoCO, CpRhCO, or CpIrCO, like $Fe(CO)_4$ (C_{2v}), as organometallic analogues of CH_2,[34] permitting simple ways of describing complex systems, where such subunits gather to form dimetallacyclopropanes, clusters, etc. Toward single-faced acceptor

(38) Hoffmann, R. *Acc. Chem. Res.* **1971**, *4*, 1.

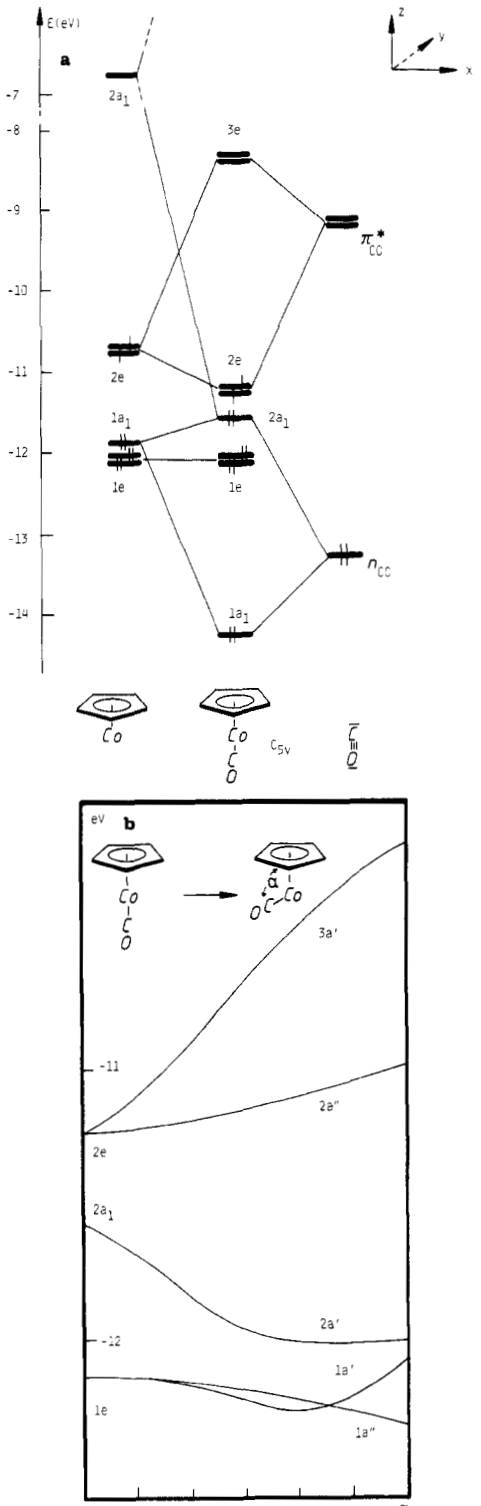

Figure 5. (a) Orbital interaction diagram for "linear" CpCoCO (C_{5v}). (b) Walsh diagram for bending C_{5v} CpCoCO to the C_s geometry.

ligands 2a″ will cause strong conformational preferences for geometries with π overlap to this rather high-lying donor level.[39] z^2 in CpCoCO is again the metal orbital that, through the stabilization of the 2a′ level, carries most of the energetic preference for bending. This time, reduced antibonding to the donor level n of CO is superimposed

(39) The computed rotational barrier for a CH_2 ligand in a model complex CpRh(CO)(CH_2) is greater than 25 kcal/mol: Hofmann, P. unpublished results.

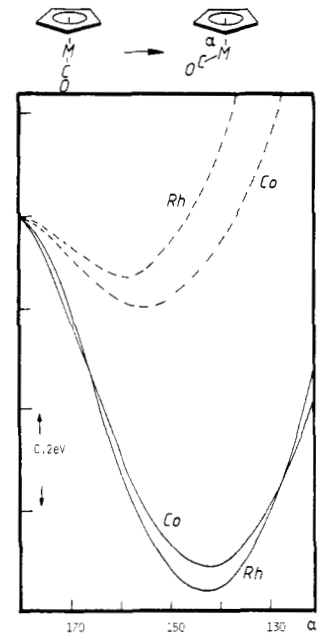

Figure 6. Total energy for bending CpCoCO and CpRhCO: solid lines, 2a″ doubly occupied; dashed lines, 3a′ and 2a″ each singly occupied.

by turning on the stabilizing interaction to a π^* acceptor orbital, as shown in **18**. As above, an avoided crossing with

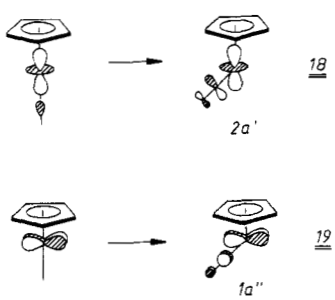

$x^2 - y^2$ (1a′) is seen in the Walsh diagram. In contrast to the pure σ-donor case, 1a″ (xy) also gets somewhat stabilized by a π^* CO component (see **19**). In simple terms one could say that the bent CpCoCO structure is better than the linear one (on the basis of one-electron MO levels) because there is improved back bonding to the ligand (via yz, z^2, and xy in C_s as opposed to only yz and xz in C_{5v}). This is clearly reflected by the computed metal charges of CpCoCO in both geometries (C_{5v}, 0.112–; C_s, 0.256) as well as in the reduced overlap populations to and within the CO group (C_{5v}, n_{Co-C} = 0.843, n_{C-O} = 1.226; C_s, n_{Co-C} = 0.908, n_{C-O} = 1.188).

The changes in total energy upon bending for the models CpCoCO and CpRhCO are shown in Figure 6 (solid lines). The bent minima for an occupation pattern $(2a'')^2$ (Co, α = 142°, stabilization 0.716 eV = 16.5 kcal; Rh, α = 142°, stabilization 0.759 eV = 17.5 kcal) correspond to a HOMO–LUMO gap of 0.62 (Co) and 0.83 eV (Rh), respectively. The dotted curves correspond to having one electron in 3a′ and 2a″. If we could compare a pure σ donor ligand with a hypothetical one of the same donor strength but with additional acceptor levels available, then the conclusion from above is that the availability of acceptor orbitals should cause a more bent structure and should increase the HOMO–LUMO gap. Model calculations on CpRh(PH_3) with and without d orbitals on P in fact show this behavior. This choice is as close as possible to adding just acceptor levels to an unaffected donor—of course, the set of d levels also causes slight changes in the lone-pair

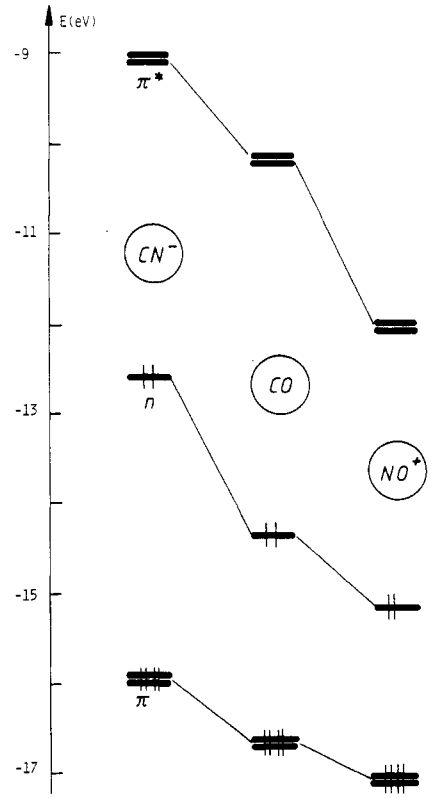

Figure 7. EH frontier orbital energies for the model ligand systems CN^-, CO, and NO^+.

orbital of PH_3, but these changes are very minor.

For real ligands, of course, σ-donating and π-accepting power are always interrelated. So when we attempt to test in calculations the influence of weak vs. strong acceptor properties (say of CN^- vs. CO) or vice versa (say of NO^+ vs. CO), we inevitably change both of these electronic features of the ligand. This is revealed by Figure 7, a sketch of the EH orbital energies of CO, CN^-, and NO^+, showing the degenerate π and π^* levels as well as the lone-pair donor orbital n of each group.

In all cases of Figure 7 the interatomic distances are taken at a constant value as we are not considering the free ligand molecules or ions but rather some geometry of the groups bound to a metal center.

Despite this interrelation of donor and acceptor propensities the trends can be discussed separately as deduced from the above CpCoL and CpCoCO cases. The consequence of a lowered π^* acceptor set would be to cause the following on bending: more destabilization of 3a′ (xz) and 2a″ (yz) due to the greater loss of back-bonding and more stabilization for 2a′ (z^2) and 1a″ (xy) due to stronger interaction with the acceptor levels. Pushing the acceptor set to higher energy will bring about the opposite effects.

In total, a better acceptor ligand L should cause a low-spin d^8 CpML to exhibit a stronger tendency to be bent but will not lead to a very improved magnitude of the HOMO–LUMO gap. We have tested this on both cobalt and rhodium analogues. Figure 8 shows the comparative features for CpRhCO, $CpRhNO^+$, and $CpRhCN^-$. The bending angle is practically the same, CpRhCO gains about 0.1 eV more in going to the C_s singlet arrangement than does $CpRhCN^-$, and bent $CpRhNO^+$ is in turn 0.2 eV more stable (relative to the linear geometry) than CpRhCO. The HOMO–LUMO gaps are 0.83, 0.82, and 0.77 eV at 142, 140, and 144°, respectively for the CO, CN^-, and NO^+ cases. The total energy curves for a situation with both 3a′ and 2a″ singly occupied show the same trend. CN^-, of course,

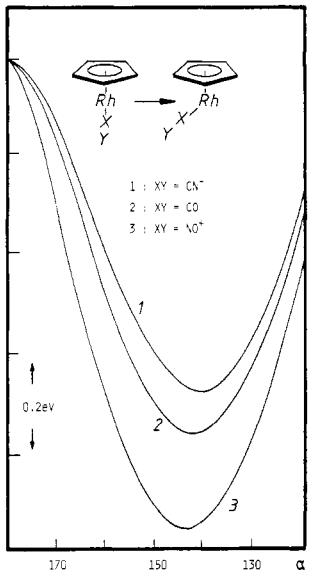

Figure 8. Total energy for $C_{5v} \rightarrow C_s$ transformations of model systems $CpCoCN^-$, CpCoCO, and $CpCoNO^+$ (2a″ doubly occupied).

also is a better σ donor than CO (see Figure 7), NO^+ is a weaker one, and this counterbalances and tempers the effects of the reduced or increased acceptor influence. Apparently, however, the changes in the ligand accepting capability dominate the picture.

It is in principle conceivable that for very strong acceptor ligands the linear C_{5v} geometry (see Figure 5a) could have the $2a_1$ level (z^2, antibonding with n) above the 2e set (xz, yz, bonding to π^*). Indeed model calculations for $CpCoNO^+$ and $CpCoNS^+$ give this sort of picture. The very small energetic separation of $2a_1$ and 2e suggests a high-spin situation for C_{5v} again. Bending to a C_s structure stabilizes the low-spin systems as found for the $2a_1$ below 2e case. The empty level $2a_1$ on bending rapidly gets destabilized, changes its character, and becomes 3a′ with predominant xz contribution, the xz member of the occupied 2e set transforms into 2a′ with dominant z^2 participation and descends in energy. In other words the inverted $2a_1$ above 2e sequence of a linear structure is immediately reversed by mutual xz/z^2 mixing (an avoided crossing) on bending. The computed reversal of the frontier levels $2a_1$ and 2e for C_{5v} $CpCoNO^+$ and $CpCoNS^+$ may well be an artifact of the specific method and parametrization we have used. Ab initio MO calculations[40] and photoelectron spectroscopic work[41] on the 18-electron system CpNiNO (C_{5v} symmetry experimentally[26]) seem to give a 2e above $2a_1$ orbital pattern for this nitrosyl compound in its ground state. It should be noted, however, that the PE assignment, based upon ΔSCF calculations, shows ionization from $2a_1$ to occur easier than from 2e. This has been interpreted as a consequence of the inapplicability of Koopmans theorem due to large orbital relaxations (about 7 eV) of the metal-centered levels. It might be though that the ground-state SCF calculation itself does not show the correct energy ordering due to the limited basis set used.

Of course for a system like CpNiNO, where $2a_1$ and 2e both are fully occupied, the energetic ordering of these two levels is irrelevant with respect to the total extent of dative bonding and back-bonding between CpNi and the NO

(40) Hillier, I. H.; Saunders. V. R. *Mol. Phys.* **1972**, *23*, 449.
(41) Evans, S.; Guest, M. F.; Hillier, I. H.; Orchard, A. F. *J.C.S., Faraday Trans. 2*, **1974**, *70*, 417. Burnier, R. C.; Freiser, B. S. *Inorg. Chem.* **1979**, *18*, 906.

ligand. For a 16-electron fragment like $CpCoNO^+$, however, the $2a_1$ above 2e pattern, leaving 2e filled and $2a_1$ empty, leads to stronger back-bonding to NO (via *xz and yz*) than the 2e above $2a_1$ orbital pattern. A rather positively charged metal center results as a consequence. Bending to a C_s geometry in the earlier discussed 2e above $2a_1$ case of CpCoCO had served to reduce the negative charge at the metal by strengthening the metal to π^* back-donation. Bending of a fragment with the $2a_1$ level above the 2e set will reduce the high positive charge, leading to comparable bonding situations in both cases for a bent low-spin minimum structure.

If we consider both σ-donating and π-accepting abilities of ligands L in d^8 CpML together, we can conclude that the best chance for such a fragment to survive on the singlet energy surface should be offered by good σ donors with additional good π-accepting capacity. The structure such species will choose to adopt will inevitably be a bent one. What we have dismissed up to now in analyzing π acceptor ligand effects is the influence of the occupied π levels of such groups. We will, however, single out the consequences of π donor levels of ligands in the next section.

d^8 CpML (L = π Donor). A typical π donor ligand would be a monoatomic group like Cl^-, carrying a set of three degenerate filled p orbitals (lone pairs). So let us take the hypothetical $CpCoCl^-$ as a model to find out what a low-lying set of filled orbitals with π symmetry toward the CpCo fragment will do within our picture.

Now according to Figure 9a the linear C_{5v} structure exhibits a large energy separation between the half-filled 2e set, destabilized by antibonding to the two appropriate p-donor orbitals of the ligand, and $2a_1$, which feels the σ-antibonding interaction to the filled s and the third p level of the attached group. Figure 9b, the total EH energy change for bending to C_s (low-spin model, 2a″ in Figure 9a doubly occupied) reveals a preference for a bent geometry again, but the total gain in energy due to orbital energy variations is only rather small (0.18 eV = 4 kcal). In $2a_1$ (z^2), which is stabilized by bending to a much lesser extent than in our earlier model systems, σ antibonding is reduced as before, but it is now replaced by π-antibonding interactions to a p-donor AO of Cl^-. The same sort of antibonding is turned on to the xy member of the C_{5v} 1e orbital. This is schematically shown in **20** and **21** and is seen in the Walsh diagram of Figure 9c. $x^2 - y^2$ as

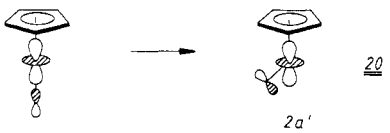

20

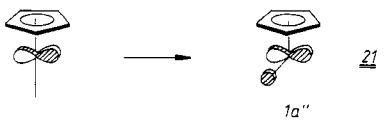

21

well is destabilized slightly by σ antibonding to the ligand. While the LUMO 3a′ (xz) of the low-spin system behaves analogously on bending as in the π acceptor ligand case, the HOMO 2a″ (yz) now even reveals a small stabilization in energy because bending reduces the overlap and the antibonding interaction to the y AO function of the halide ligand as shown in **22**.

22

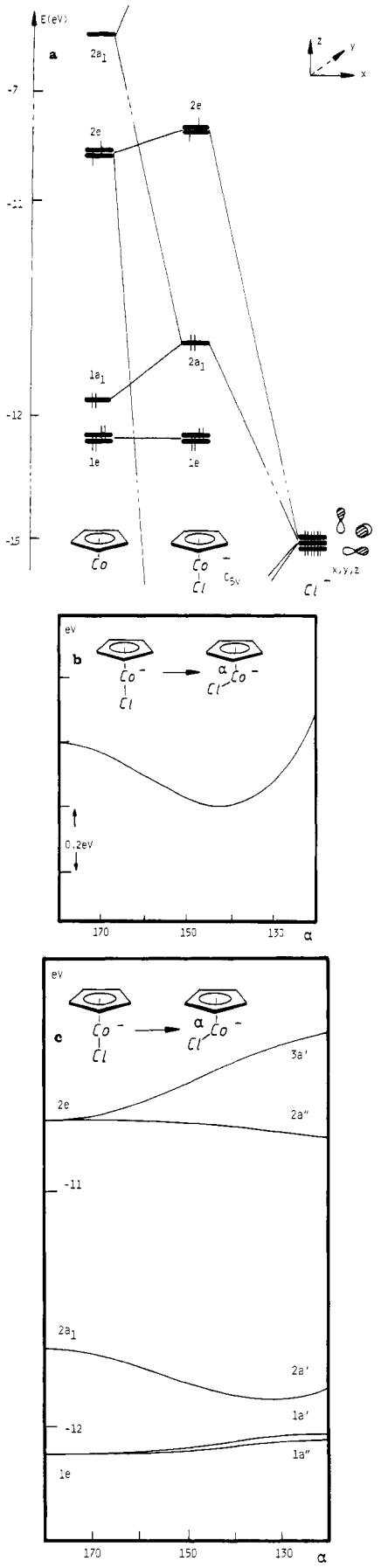

Figure 9. (a) Interaction diagram for $CpCoCl^-$ (C_{5v}). (b) Total energy for bending $CpCoCl^-$ (2a″ doubly occupied). (c) Corresponding Walsh diagram.

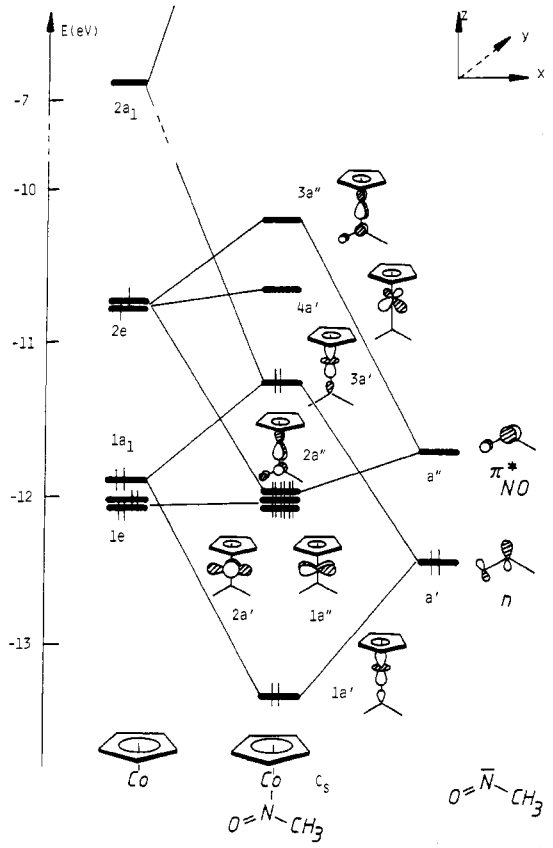

Figure 10. Orbital interaction diagram for "linear" (C_s) CpCo(CH_3NO), **24**.

Generally we can conclude that π-donating character on L will lead to a rather small energetic preference for a bent structure if a low-spin situation is simulated by placing two electrons in 2a''. The developing HOMO–LUMO gap is not big, and the chance for a bent singlet system is not high. Putting one electron each in 3a' and 2a'' makes the tendency to bend practically vanish.

To summarize at this point, d^8 CpML intermediates with 16 valence electrons especially for the heavier metals may well have singlet ground-state structures and will be bent in particular if the metal bound ligands L are good σ donors and, in addition, possess π acceptor capabilities. This may well explain the nonexistence of a high energy barrier due to spin forbiddeness in Bergman's experiment involving dissocation of $CpCo(PPh_3)_2$ to form $CpCo(PPh_3)$ as an intermediate in the substitution process. The thermal equilibrium of $CpIr(CO)H_2$ and $CpIr(CO) + H_2$ was well as the other observations cited in the beginning could become understandable then as well.

We would like to point out here that the oxidative addition of H_2 or a C–H bond to a bent singlet d^8 CpML is an allowed ground-state process. This is easily derived from a Woodward–Hoffmann type correlation diagram (orbital or state correlation) for this reaction. In contrast to the isolobal carbene case, where the symmetric least motion insertion into the H_2 bond is forbidden, a d^8 CpML singlet system with a bent Cp–M–L arrangement has the antisymmetric valence level (2a'') occupied and the σ-type level (3a') empty, leading to the necessary HOMO–LUMO interactions for the least motion insertion reaction.

If d^8 CpML 16-electron fragments are generated in an initial triplet state in photochemical experiments, intersystem crossing, which becomes possible for such heavy-atom molecules, can nevertheless lead to a bent singlet intermediate and to subsequent ground-state chemistry of that species, if the singlet is lowest in energy as our analysis of bent CpML fragments indicates.

It would be extremely interesting to see the conclusions of our qualitative analysis being tested by "state of the art" ab initio calculations, and we hope to hereby encourage such studies, which then however would have to involve large enough basis sets, extensive geometry optimizations, and an appropriate amount of correlation.[42]

CpCo(O=NCH$_3$), a d^8 CpML Fragment (L = Single-Faced Acceptor). We close our analysis by inspecting the fragment $CpCo(NOCH_3)$, **9**, which has been identified as an intermediate by Bergman et al. in their study of the NO insertion reaction **8** → **10**.[23] This case is particularly interesting because not only do we have here a single-faced π-acceptor ligand, the nitrosomethane fragment **23** but also

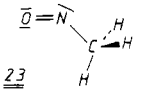

23

because several conceivable different ground-state structures come into question for **9**. The CH_3NO ligand may be bound in a η^1 fashion via nitrogen, as found in the X-ray structure of **10**, the isolated phosphine adduct of **9**, with a possibility of giving four alternative structures of linear or bent geometry (**24**–**27**). The η^1-bonding mode is also frequently but not exclusively found for metal-bound acyl groups RCO. **25** and **26** can be derived from the linear

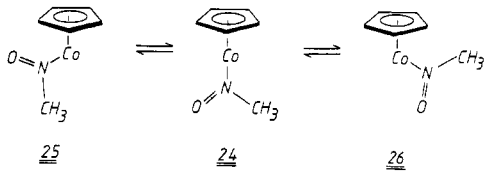

25 **24** **26**

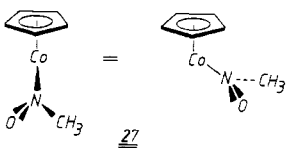

27

geometry **24** by bending within the Co–CH_3NO plane toward either the oxygen or the methyl side, and **27** results from bending **24** perpendicular to the Co–CH_3NO plane or, alternatively, from a 90° rotation around the Co–N bond in **25** or **26**. Figure 10 presents the computed interaction diagram between a CpCo fragment and the CH_3NO ligand for the geometric arrangement as in linear **24**. At the ligand, two frontier orbitals are relevant, the donor orbital n, localized more at nitrogen with some antibonding p contribution from oxygen and the low-lying π^*_{NO} acceptor level of the N=O double bond. The HOMO of **24** derives from $1a_1$ (z^2) of CpCo, which is destabilized by n of the ligand (again the high-lying $2a_1$ orbital of CpCo mixes into this level in a bonding way). The xy and $x^2 - y^2$ levels (1e of CpCo) of the metal are practically unaffected by the ligand. The xz member of 2e of the metal fragment does not feel much ligand interaction either and stays put. The reader will so far have recognized exactly our old pure σ donor case discussed earlier. The important additional interaction for **24** stems from π^*_{NO} of CH_3NO and the yz member of 2e. The bonding combination of these two levels, due to the low energy of π^*_{NO}, is found close above xy and $x^2 - y^2$ of the metal, far below z^2. This level is occupied by two electrons, and thus the picture corresponds to the $2a_1$ above 2e situation that we have

(42) Veillard, A.; Dedieu, A., some ab initio work on CpRhCO, submitted for publication in *Theor. Chim. Acta*.

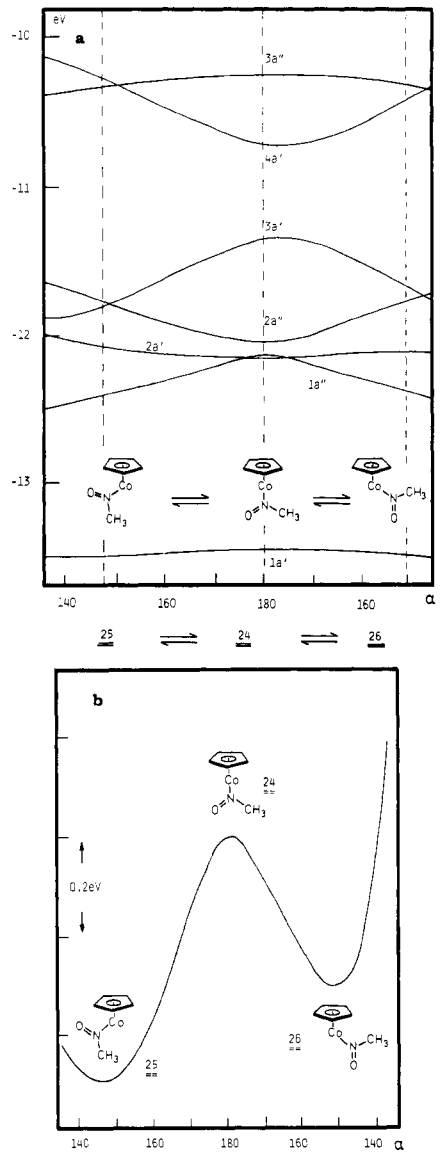

Figure 11. (a) Walsh diagram for transforming **24** into **25** (left) and **26** (right) and (b) corresponding total energy behavior.

described for strong double-faced π accceptors before. A HOMO–LUMO gap of about 0.75 eV is found already for such a linear structure **24** of CpCo(CH_3NO). From what we have learned about the simplified model systems in the earlier sections, it is clear that **24** will have an electronic tendency to also adopt a bent geometry, either **25**, **26**, or **27**. Bending in any case will stabilize the z^2-derived HOMO by reducing the antibonding to n, and this is seen in Figure 11a, the Walsh diagram for transforming **24** into **25** (left) or **26** (right). For these two geometries the xz level (4a′) of the linear form is going up in energy as in all other cases before. The highest empty level shown in Figure 11a, 3a″ (yz) of CpCo antibonding to π^*_{NO}, is going down slightly for the same reason that causes the π^*_{NO} + yz (2a″) MO to go up and counteract the stabilization of z^2. The x^2-y^2-based orbital (2a′) gets somewhat destabilized while xy starts to interact with π^*_{NO} and gains in energy. According to Figure 11b both bent structures **25** (α = 147°) and **26** (α = 150°) are energetically better than **24**. **25** is preferred by about 0.17 eV over **26**, and this slight preference is mainly a result of steric factors and of the somewhat differing overlap situation of z^2 with n for the two ligand orientations in **25** and **26**, leading to a lower lying z^2-type level in **25**. The HOMO–LUMO gap for the

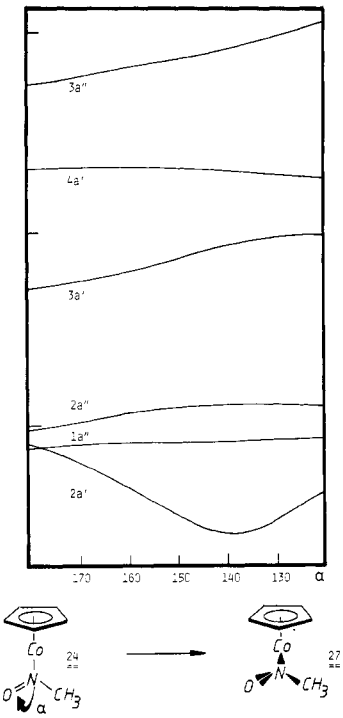

Figure 12. Frontier level Walsh diagram for going from **24** to **27**. The frontier levels alone, as shown in the figure, still would induce some gain in total energy on bending to **27**. The overall loss in energy for going from **24** to **27** is mainly due to a series of lower lying levels not included in the diagram.

two bent geometries, where the two lowest empty levels derived from xz and yz at the metal become nearly degenerate, increases to 1.5 eV. This gap, within the EH framework of theory, ensures a singlet ground state for such bent CpCo(CH_3NO) 16-electron intermediates and indicates that reactions via such species can take place without problems on the singlet energy surface.

Transforming linear CpCo(CH_3NO) (**24**) to the bent geometry **27** is found to be unfavorable. From the MOs of **24**, displayed schematically in Figure 10, the reader can easily see that bending perpendicular to the Co–ligand plane will leave the LUMO (xz) unaffected and will reduce the π interaction between yz and π^*_{NO}, replacing it by σ antibonding of yz to n. Bending of **24** toward **27** also induces π interaction of z^2 with π^*_{NO}. This causes the HOMO of **24** not to descend in energy because now the stabilization due to reduced antibonding to n of the ligand is undone by the mixing of π^*_{NO} into z^2 in an antibonding fashion. It is only the bonding combination of z^2 and π^*_{NO} which is stabilized upon going from **24** toward **27**. Figure 12 displays the energy level changes for this geometric distortion. In contrast to the stable bent structures **25** or **26** bent **27** has a smaller gap between HOMO and LUMO than even linear **24**. This is also easily derived if one goes to **27** by rotation around the Co–N bond of either **25** or **26**. To follow this can be left to the reader.

So far we have kept the CH_3NO ligand bound to Co in a η^1 manner. In fact it is well-known that in various stable and isolable acyl complexes of transition metals electronic unsaturation at the metal center is circumvented by coordinating acyl groups in a η^2 way[43] (see **28**). This has been

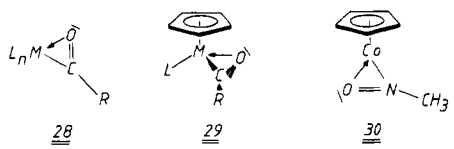

Table II. Extended Hückel Parameters

orbital	H_{ii}, eV	ζ_1	ζ_2	c_1[a]	c_2[a]
Co 3d	−12.11	5.55	2.1	0.567 86	0.605 68
4s	−8.54	2.0			
4p	−4.76	2.0			
Rh 4d	−13.6	4.29	1.97	0.580 70	0.568 50
5s	−8.77	2.135			
5p	−5.20	2.10			
H[b] 1s	−13.6	1.3			
P 3s	−18.6	1.6			
3p	−14.0	1.6			
3d	−7.0	1.4			
Cl 3s	−30.0	2.033			
3p	−15.0	2.033			

[a] Coefficients in the double-ζ expansion. [b] Both H_{ii} value and 1s exponent were varied to mimic a change in σ-donor ability. For explanation see text.

discussed also as one possibility to explain the stereochemical behavior of 16-electron intermediates of the CpML(acyl) type like **29**.[44] For $CpCo(CH_3NO)$ this might suggest a structure like **30**. Indeed our calculations reveal **30** (with an idealized, symmetric[45] ligand arrangement) to be of comparable energy to the bent η^1 species **25** and to also have a large HOMO–LUMO gap of about 1.2 eV. The HOMO now is the antibonding combination of xy and π^*_{NO}, shown in **31**. The LUMO, **32**, results from antibonding of π^*_{NO} with yz. The oxygen lone pair fills the

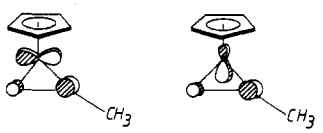

31 32

valence shell of the cobalt atom, and **30** in our calculations finds its minimum energy with a "planar" ligand arrangement as generally found for $CpML_2$ 18-electron complexes, e.g., $CpCo(CO)_2$, $CpCo(PR_3)_2$, etc. We hesitate, however, to assign a relative energy ordering to the two stable minimum structures of $CpCo(CH_3NO)$ (**9**), because the η^2 structure would require optimization of at least some of the bond lengths. This cannot be done reliably within the EH model. In any case, an intermediate d^8 $CpM(CH_3NO)$ should be a system with a singlet ground state.

Conclusions

Qualitative MO theory, supported by EH calculations, shows that 16-electron intermediates d^8 CpML with appropriate ligands can adopt bent (C_s) singlet structures in their electronic ground state. Especially good candidates for bent singlet structures ares systems with good σ-donating, π-acceptor ligands and with the heavier metal atoms. Many reactions, where such species have been invoked as essential intermediates formed by thermal or photochemical ligand dissociations or by other routes, can thus proceed on the singlet energy surface without any spin-induced barriers.

Acknowledgment. We are grateful to the Deutsche Forschungsgemeinschaft and to the Fonds der Chemischen Industrie for generous support of this work. The cooperation of the staff of the Regionales Rechenzentrum der Universität Erlangen is also gratefully acknowledged. We thank Prof. Roald Hoffmann and Dr. B. E. R. Schilling for helpful discussions and Prof. A. Veillard and Dr. A. Dedieu for providing results of their work prior to publication.

Appendix

The parameters used in the extended Hückel calculations are given in Table II. The modified Wolfsberg–Helmholz formula was used throughout the calculations.[46] H_{ii} values for cobalt as well as wave functions were taken from earlier work,[47] H_{ii} values for Rh were obtained from charge-iterative calculations on $CpRh(CO)_2$, and the Rh orbital exponents are those used in previous work.[48] The main-group parameters are standard ones. To model weak and strong donors the 1s H_{ii} of hydrogen (the L model ligand) was modified as indicated in the main body of the paper. P was considered with and without d functions.

Idealized C–C (1.41 Å) and C–H distances (1.09 Å) were taken for the Cp groups in all cases. The $Co–C_{Cp}$ and $Rh–C_{Cp}$ distances were 2.088 and 2.25 Å, respectively. The Co–CO distance was taken as 1.728 Å, and the same value was employed for Co–CN and Co–NO to compare these ligand types rationally. For the Rh analogues these distances were set at 1.83 Å. On similar grounds the C–O, C–N, and N–O distances in all the diatomic ligands were kept constant at 1.135 Å. The other distances used were Co–H = 1.556 Å, Co–P = 2.145 Å, $Co–CH_3$ = 2.0 Å, Co–Cl = 2.3 Å, Rh–H = 1.72 Å, Rh–P = 2.30 Å, $Rh–CH_3$ = 2.1 Å, and Rh–Cl = 2.37 Å. For the nitrosomethane complex **9** the bond distances were adapted from its PPh_3-containing analogue reported in ref 23.

Registry No. $CpCo(PH_3)$, 86803-00-1; $CpRh(PH_3)$, 86803-01-2; $CpCo(CH_3)^-$, 86803-02-3; $CpRh(CH_3)^-$, 86803-03-4; CpCoCO, 73740-50-8; CpRhCO, 86803-04-5; $CpCoCN^-$, 86803-05-6; $CpCoNO^+$, 86803-06-7; $CpCoCl^-$, 86803-07-8; $CpCo(CH_3NO)$, 86803-08-9.

(43) Fachinetti, G.; Floriani, C. *J. Organomet. Chem.* **1974**, *71*, C5. Fachinetti, G.; Floriani, C.; Stoeckli-Evans, H. *J. Chem. Soc., Dalton Trans.* **1977**, 2297. Fachinetti, G.; Floriani, C.; Marchetti, F.; Merlino, S. *J. Chem. Soc., Chem. Commun.* **1976**, 522. Fachinetti, G.; Fochi, G.; Floriani, C. *J. Chem. Soc., Dalton Trans.* **1977**, 1946. Fagan, P. J.; Manriquez, J. M.; Marks, T. J.; Day, V. W.; Vollmer, S. H.; Day, C. S. *J. Am. Chem. Soc.* **1980**, *102*, 5393. Fagan, P. J.; Manriquez, J. M.; Vollmer, S. H.; Day, C. S.; Marks, T. J. *Ibid.* **1981**, *183*, 2206. Franke, U.; Weiss, E. *J. Organomet. Chem.* **1979**, *165*, 329.

(44) Brunner, H.; Vogt, H. *Angew. Chem.* **1981**, *93*, 409. *Angew. Chem., Int. Ed. Engl.* **1981**, *20*, 405. Brunner, H.; Vogt, H. *Chem. Ber.* **1981**, *114*, 2186 and references therein.

(45) Equal bond distances from Co to N and O, angle O–N–C being 120°.

(46) Ammeter, J. H.; Bürgi, H.-B.; Thibeault, J. C.; Hoffmann, R. *J. Am. Chem. Soc.* **1978**, *100*, 3686.

(47) Albright, T. A.; Hofmann, P.; Hoffmann, R. *J. Am. Chem. Soc.* **1977**, *99*, 7546.

(48) Summerville, R. H.; Hoffmann, R. *J. Am. Chem. Soc.* **1976**, *98*, 7240.